

Maxwell's Equations in Anisotropic Materials: Half-Waveplates, Quarter-Waveplates, and Uniaxial Media

KEVIN LINDSTROM^{1,*}

¹ Graduate Student, Department of Electrical and Computer Engineering, University of Connecticut, 371 Fairfield Way, Storrs, CT 06269-4157, USA.

*kevin.lindstrom@uconn.edu

Abstract: This paper discusses electromagnetic in uniaxial media and focuses on the specific case of designing a waveplate. Waveplates are useful optical devices that change the polarization of an incident electromagnetic wave and are used in many applications from research to photography. This report covers the necessary theoretical background that describes electromagnetic fields in anisotropic materials, and derives series solutions for the output fields of a simple half-waveplate and quarter-waveplate. These analytical solutions were then used to design these waveplates using a quartz crystal for 590 nm normally incident light. The performance of the designed waveplates was evaluated, and oblique incidence was discussed. Design challenges surrounding waveplate design were mentioned as well.

© 2023 Optica Publishing Group

Contents

1	Introduction	1
2	Theory	2
2.1	The Displacement Field	2
2.2	Anisotropy and The Displacement Field	3
2.3	Uniaxial Media	3
2.4	The Wave Equation in Uniaxial Media	4
2.5	Normal Incidence	5
3	Design	6
3.1	Half-Waveplate Design	6
3.2	Quarter-Waveplate Design	8
3.3	Designed Waveplates	9
4	Discussion	11
4.1	Oblique Incidence	11
4.2	Anti-Reflective Coatings	14
4.3	Wavelength Dependence	14
4.4	Liquid Crystals	15
5	Conclusion	15

1. Introduction

Describing electromagnetic waves in anisotropic material is of practical interest for describing designing many optical devices that are useful in research as well as the wider economy. This report will investigate a Maxwell's Equation based approach to modelling light in an anisotropic

material and will design a simple quartz half-waveplate (HWP) and quarter-waveplate (QWP) with this approach. Anisotropic materials are materials that have directional dependence to their constitutive parameters. Our discussion will primarily focus on plane wave incidence on a birefringent material that has a “fast” and “slow” optical axis. This nomenclature will be explained later on in the report. We will start with the theoretical background that introduces the math necessary to perform the design and analysis. It will be shown that for uniaxial anisotropic media that the \hat{x} , \hat{y} , and \hat{z} components of the wave equation remain uncoupled, and that this allows fields in \hat{x} and \hat{y} to propagate in \hat{z} independent of each other.

We will now have a brief aside about notation. In this report, most vectors will be denoted by a bold variable, for example the electric field phasor $\mathbf{E}(x, y, z)$ and the unit vector \hat{x} . Time varying fields, however, will be denoted by a script with a vector mark $\vec{\mathcal{E}}(x, y, z; t)$. Furthermore, matrices will be denoted by a simple bar over the variable, like the dielectric matrix $\bar{\epsilon}$. Additional notation will be explained when necessary.

2. Theory

The theory will be introduced from the most general to the specific such that the assumptions necessary for the waveplate design are well substantiated, and the reader will be able to grasp more complex anisotropic materials that will be lightly discussed later in the report. We begin our discussion with the displacement field $\vec{\mathcal{D}}(x, y, z; t)$.

2.1. The Displacement Field

As is discussed in *Advanced Engineering Electromagnetics* time varying fields can be analyzed in the phasor domain if they are time harmonic, and the relationship between the time domain and phasor domain is as follows (shown in Cartesian coordinates for clarity)

$$\vec{\mathcal{D}}(x, y, z; t) = \Re \{ e^{j\omega t} \mathbf{D}(x, y, z) \} \quad (1)$$

where ω is the angular frequency of the time harmonic field [1]. The displacement field $\vec{\mathcal{D}}(x, y, z; t)$ is a useful tool for analyzing the electric field in media and has units of $C \cdot m^{-2}$. It has the following relationship to the electric field $\vec{\mathcal{E}}(x, y, z; t)$ for isotropic media (media without directional dependent constitutive parameters)

$$\vec{\mathcal{D}}(x, y, z; t) = \epsilon_0 \vec{\mathcal{E}}(x, y, z; t) + \vec{\mathcal{P}}(x, y, z; t) = \epsilon \vec{\mathcal{E}}(x, y, z; t) \quad (2)$$

where $\vec{\mathcal{P}}(x, y, z; t)$ is the polarization of the material—not to be confused with the polarization of an electromagnetic (EM) wave. The above relationship holds true in the phasor domain as well

$$\mathbf{D}(x, y, z) = \epsilon_0 \mathbf{E}(x, y, z) + \mathbf{P}(x, y, z) = \epsilon \mathbf{E}(x, y, z) \quad (3)$$

where in both Equation (2) and (3) the material’s permittivity ϵ can be related to its relative permittivity ϵ_r [2]

$$\epsilon = \epsilon_0 \epsilon_r \quad (4)$$

At an interface from material 1 to 2, the parallel and perpendicular boundary conditions (BC) for the displacement field are

$$(\mathbf{D}_2 - \mathbf{D}_1) \cdot \hat{\mathbf{n}}_{12} = \sigma_f \quad \text{and} \quad (\mathbf{D}_2 - \mathbf{D}_1) \times \hat{\mathbf{n}}_{12} = (\mathbf{P}_2 - \mathbf{P}_1) \times \hat{\mathbf{n}}_{12} \quad (5)$$

respectively, where σ_f is the free (unbounded) surface charge density at the interface, and $\hat{\mathbf{n}}_{12}$ is the normal vector of the interface from medium 1 to medium 2 [2]. These relationships are the same as saying that the tangential components of the electric field must be continuous at a dielectric-dielectric interface. Now that we have introduced the displacement field, we now discuss the displacement field in anisotropic media.

2.2. Anisotropy and The Displacement Field

Anisotropic materials are materials that are directional dependent, and for our discussion we will consider the case of directional dependence of the material's permittivity. Many materials in nature have this dependence as their crystalline structure creates many small dipole moments that affect the material's polarization. In the most broad sense, an anisotropic material's relative permittivity can be written as a rank 2 tensor (a matrix) [1, 3, 4]

$$\bar{\epsilon}_r = \begin{bmatrix} \epsilon_{xx} & \epsilon_{xy} & \epsilon_{xz} \\ \epsilon_{yx} & \epsilon_{yy} & \epsilon_{yz} \\ \epsilon_{zx} & \epsilon_{zy} & \epsilon_{zz} \end{bmatrix} \quad \text{where } \epsilon_{ij} = \epsilon_{ji}^* \quad (6)$$

Equation (3) then becomes

$$\mathbf{D}(x, y, z) = \epsilon_0 \bar{\epsilon}_r \mathbf{E}(x, y, z) \quad (7)$$

So we see that the displacement field in \hat{x} obtains components from the electric field in \hat{y} and \hat{z} in addition to \hat{x}

$$D_x = \epsilon_0 (\epsilon_{xx} E_x + \epsilon_{xy} E_y + \epsilon_{xz} E_z) \quad (8)$$

In Equation (6) it was stated that $\epsilon_{ij} = \epsilon_{ji}^*$ which is equivalent to saying $\epsilon_r = \epsilon_r^\dagger$ where the \dagger operator indicates complex conjugate transpose. This means that the permittivity tensor is a Hermitian matrix if it is complex, and is plainly symmetric if it is purely real! It should be fairly clear that this should be expected behavior of an anisotropic material. We would expect that a contribution to D_x by E_z would be the conjugate to a contribution to D_z by E_x because the waves would be interacting with the same segment of the material's crystalline structure. It should be noted that for materials with cross terms in their permittivity tensor (ϵ_{xy} , ϵ_{zx} , etc.), it is not possible to craft the wave equation. The respective fields in each direction are coupled with each other, so analyzing materials with cross terms, like liquid crystals, is a bit more involved. Consequently, we will begin our discussion of uniaxial media.

2.3. Uniaxial Media

Uniaxial media are a special case of anisotropic media that have two different permittivities which depend on the orientation of the material. They have one direction where their permittivity is characterized by the extraordinary permittivity ϵ^e and the two other directions are characterized by the ordinary permittivity ϵ^o . If the coordinate system is chosen such that it aligns with these crystalline axes, called the extraordinary axis and ordinary axes a uniaxial material's permittivity tensor can take the form

$$\bar{\epsilon}_r = \begin{bmatrix} \epsilon^e & 0 & 0 \\ 0 & \epsilon^o & 0 \\ 0 & 0 & \epsilon^o \end{bmatrix} \quad (9)$$

where the \hat{x} axis was chosen to be the extraordinary axis such that \hat{y} and \hat{z} are ordinary [4]. This choice was made such that our theoretical discussion matches our desired design because we will be looking for devices that have \hat{z} plane-wave incidence. With the given permittivity matrix, it should be seen that Equation (7) yields

$$\begin{cases} D_x = \epsilon_0 \epsilon^e E_x \\ D_y = \epsilon_0 \epsilon^o E_y \\ D_z = \epsilon_0 \epsilon^o E_z \end{cases} \quad (10)$$

where the displacement fields in \hat{x} , \hat{y} , and \hat{z} are independent.

2.4. The Wave Equation in Uniaxial Media

Now that we have introduced the dielectric permittivity tensor for a uniaxial medium, the displacement field, and the BC of the displacement field, we can now use these concepts to derive the wave equation for time harmonic fields that describes \mathbf{E} fields inside the medium, which we are assuming is lossless and non-magnetic (good assumptions for quartz). With \mathbf{E} , \mathbf{D} , and \mathbf{H} all as functions of x , y , and z we use Faraday's Law

$$\nabla \times \mathbf{E} = -j\omega\mu_0\mathbf{H} \quad (11)$$

Ampere's Law with the current density $\mathbf{J} = \vec{0}$,

$$\nabla \times \mathbf{H} = j\omega\mathbf{D} \quad (12)$$

and Equation (7) to obtain

$$\nabla \times \nabla \times \mathbf{E} = -j\omega\mu_0\nabla \times \mathbf{H} = \omega^2\mu_0\mathbf{D} \quad (13)$$

[1, 4]. We then use

$$\nabla \times \nabla \times \mathbf{E} = \nabla(\nabla \cdot \mathbf{E}) - \nabla^2\mathbf{E} = -\nabla^2\mathbf{E}$$

to obtain the wave equation

$$\nabla^2\mathbf{E} + \omega^2\mu_0\mathbf{D} = \nabla^2\mathbf{E} + \omega^2\mu_0\epsilon_0\bar{\epsilon}_r\mathbf{E} = 0 \quad (14)$$

We demonstrated that for the given uniaxial material with permittivity tensor $\bar{\epsilon}_r$ that D_x , D_y , and D_z are uncoupled so Equation (14) can be rewritten as

$$\begin{cases} \frac{\partial^2 E_x}{\partial x^2} + \omega^2\mu_0\epsilon_0\epsilon^e E_x = 0 \\ \frac{\partial^2 E_y}{\partial y^2} + \omega^2\mu_0\epsilon_0\epsilon^o E_y = 0 \\ \frac{\partial^2 E_z}{\partial z^2} + \omega^2\mu_0\epsilon_0\epsilon^o E_z = 0 \end{cases} \quad (15)$$

As is discussed in *Advanced Engineering Electromagnetics*, for each of these independent equations we choose

$$\beta^2 = \omega^2\mu_0\epsilon_0\epsilon_r$$

[1]. For the extraordinary axis (\hat{x}), we obtain

$$\beta^e = \omega\sqrt{\mu_0\epsilon_0\epsilon^e} \quad (16)$$

Likewise, we obtain

$$\beta^o = \omega\sqrt{\mu_0\epsilon_0\epsilon^o} \quad (17)$$

for the two ordinary axes [1, 4]. Because our material's permeability is not directionally dependent, it similarly obtains two impedances as shown below

$$\eta^e = \sqrt{\frac{\mu_0}{\epsilon_0\epsilon^e}} \quad \text{and} \quad \eta^o = \sqrt{\frac{\mu_0}{\epsilon_0\epsilon^o}} \quad (18)$$

These equations show that a plane wave propagating in the \hat{z} direction with \hat{y} polarization is described as

$$\mathbf{E}_{\hat{y}}(z) = \hat{y}E_0 e^{-j\beta^o z} \quad (19)$$

and a wave polarized in \hat{x} is

$$\mathbf{E}_{\hat{x}}(z) = \hat{x}E_0 e^{-j\beta^e z} \quad (20)$$

where E_0 is simply the amplitude of the electric field. Applying Equation (18) yields the respective magnetic fields [1]

$$\mathbf{H}_{\hat{\mathbf{y}}}(z) = \frac{\mathbf{E}_{\hat{\mathbf{y}}}(z)}{\eta^o} = \hat{\mathbf{y}} \frac{E_0}{\eta^o} e^{-j\beta^o z} \quad (21)$$

$$\mathbf{H}_{\hat{\mathbf{x}}}(z) = \frac{\mathbf{E}_{\hat{\mathbf{x}}}(z)}{\eta^e} = \hat{\mathbf{x}} \frac{E_0}{\eta^e} e^{-j\beta^e z} \quad (22)$$

It is demonstrated that $\mathbf{E}_{\hat{\mathbf{y}}}(z)$ and $\mathbf{H}_{\hat{\mathbf{y}}}(z)$ as well as $\mathbf{E}_{\hat{\mathbf{x}}}(z)$ and $\mathbf{H}_{\hat{\mathbf{x}}}(z)$ are in phase with each other. Consequently, the fields inside the material are not evanescent and do in fact propagate. However, because $\beta^o \neq \beta^e$, we see that the speed of propagation through the material is not the same! This is why some call the axes the fast and slow axes. In the design section of the report, we will substantiate how we can leverage this opportunity to design waveplates. Before that, we will cover normal incidence with the given uniaxial material with the permittivity tensor $\bar{\epsilon}_r$.

2.5. Normal Incidence

Suppose we have plane wave normal incidence from air (ϵ_0, μ_0) onto our specified material ($\bar{\epsilon}_r, \mu_0$) with the interface boundary at $z = 0$. The incident plane wave is given by

$$\mathbf{E}^i(z) = \frac{E_0}{\sqrt{2}} [\hat{\mathbf{x}} + \hat{\mathbf{y}}] e^{-j\beta_0 z} \quad (23)$$

where $\beta_0 = \omega\sqrt{\mu_0\epsilon_0}$. It can be seen that applying the reflection Γ and transmission T coefficients as described in *Advanced Engineering Electromagnetics* would simply not suffice. This is because the impedance of the material takes two different values depending on the direction of the field. Consequently, we have two different reflection and transmission coefficients, one for each optical axis, shown below

$$\Gamma^e = \frac{\eta^e - \eta_0}{\eta^e + \eta_0} \quad \text{and} \quad \Gamma^o = \frac{\eta^o - \eta_0}{\eta^o + \eta_0} \quad (24)$$

$$T^e = \frac{2\eta^e}{\eta^e + \eta_0} \quad \text{and} \quad T^o = \frac{2\eta^o}{\eta^o + \eta_0} \quad (25)$$

When we compute the transmitted and reflected components, we find the transmitted field

$$\mathbf{E}^t(z) = \frac{E_0}{\sqrt{2}} [\hat{\mathbf{x}} T^e e^{-j\beta^e z} + \hat{\mathbf{y}} T^o e^{-j\beta^o z}] \quad (26)$$

and the reflected field

$$\mathbf{E}^r(z) = \frac{E_0}{\sqrt{2}} [\hat{\mathbf{x}} \Gamma^e + \hat{\mathbf{y}} \Gamma^o] e^{j\beta_0 z} \quad (27)$$

As is required, the continuity of the tangential fields across the boundary is maintained

$$[\mathbf{E}^i(z=0) + \mathbf{E}^r(z=0)] \times \hat{\mathbf{z}} = \mathbf{E}^t(z=0) \times \hat{\mathbf{z}} \quad (28)$$

$$[\mathbf{H}^i(z=0) + \mathbf{H}^r(z=0)] \times \hat{\mathbf{z}} = \mathbf{H}^t(z=0) \times \hat{\mathbf{z}} \quad (29)$$

We have therefore demonstrated that the techniques described in *Advanced Engineering Electromagnetics* are compatible with our uniaxial anisotropic material, with a few extra quirks [1]. As such, we will now begin the design portion of this report.

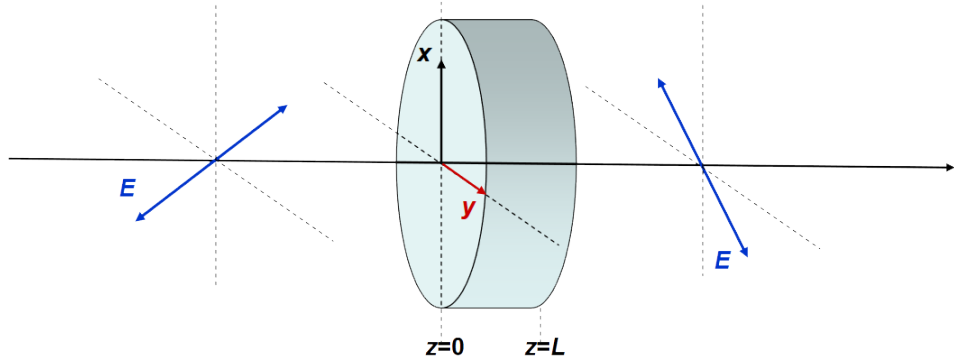


Fig. 1. A waveplate in the xy -plane with length L with an incident plane wave at $z = 0$ [4]. We choose $z < 0$ to be region 1, $0 < z < L$ to be region 2, and $z > L$ to be region 3. The blue lines indicate the polarization of the incident field \mathbf{E}_1^i and the intended polarization of the output field \mathbf{E}_3 for a HWP. The HWP should rotate the polarization of the input field by 90° .

3. Design

A HWP and QWP will be designed using the equations outlined in the theory section of this report. Figure 1 outlines the coordinate system and location of the waveplates that will be designed, and also shows the intended polarization of the incident and transmitted fields for a HWP. This diagram will be reused to design a QWP, but the designed L and the intended output polarization will be different.

3.1. Half-Waveplate Design

By inspection, it was already shown in Equations (23), (26) that linearly polarized (LP) incident light in either purely $\hat{\mathbf{x}}$ or $\hat{\mathbf{y}}$ would stay linearly polarized inside the anisotropic device and if the process was repeated for the second boundary at $z = L$ it would be seen that the output field maintains the same polarization at the input field. We will see that one possible design for a HWP uses the fact that the fields in the $\hat{\mathbf{x}}$ and $\hat{\mathbf{y}}$ directions travel at different speeds in the anisotropic medium to cause a π phase shift on one of the axes such that the output field \mathbf{E}_3 would be polarized in $(-\hat{\mathbf{x}} + \hat{\mathbf{y}})/\sqrt{2}$ if the incident light \mathbf{E}_1 was polarized in $(\hat{\mathbf{x}} + \hat{\mathbf{y}})/\sqrt{2}$.

We have already shown that an incident field propagating in $+z$ LP in the $(\hat{\mathbf{x}} + \hat{\mathbf{y}})/\sqrt{2}$ direction becomes

$$\mathbf{E}_2^t(z) = \frac{E_0}{\sqrt{2}} [\hat{\mathbf{x}} T_{12}^e e^{-j\beta^e z} + \hat{\mathbf{y}} T_{12}^o e^{-j\beta^o z}] \quad (30)$$

inside the uniaxial medium. Here we will use the subscript to denote which medium the EM wave is in, and the superscript to denote the boundaries that the EM wave has crossed. Now, if we want to find the case where the $\hat{\mathbf{x}}$ component of the electric field becomes $-\hat{\mathbf{x}}$, at the second boundary $z = L$, we can choose

$$L(\beta^e - \beta^o) = (2m + 1)\pi \quad \text{for } \forall m \in \mathbb{Z} \quad (31)$$

where \mathbb{Z} is the set of all integers [4]. When we rearrange Equation (31) we obtain a relationship which we can use to rewrite Equation (30)

$$L\beta^e = (2m + 1)\pi + L\beta^o$$

So the field in the device at $z = L$ becomes

$$\mathbf{E}_2^t(z) = \frac{E_0}{\sqrt{2}} e^{-j\beta^o L} [\hat{\mathbf{x}} T_{12}^e e^{-j(2m+1)\pi} + \hat{\mathbf{y}} T_{12}^o] = \frac{E_0}{\sqrt{2}} e^{-j\beta^o L} [-\hat{\mathbf{x}} T_{12}^e + \hat{\mathbf{y}} T_{12}^o] \quad (32)$$

When we consider the transmission on the second boundary we obtain that the transmitted field at the output \mathbf{E}_3^{tt} becomes

$$\mathbf{E}_3^{tt}(z) = \frac{E_0}{\sqrt{2}} e^{-j\beta^o L} [-\hat{\mathbf{x}} T_{12}^e T_{23}^e + \hat{\mathbf{y}} T_{12}^o T_{23}^o] e^{-j\beta_0(z-L)} \quad (33)$$

We see that our device does impart a phase shift of $\beta^o L$ on the output field but this not a concern if we are focused on just the polarization. However, what is a concern is the transmission coefficients. It should be noted that if $T^e = T^o$, then our device has no axis dependent phase retarding properties. This is because of the definition of the transmission coefficient

$$T_{12} = \frac{2\eta_2}{\eta_1 + \eta_2}$$

If we had $T^e = T^o$, it would imply $\epsilon^e = \epsilon^o$ and consequently $\beta^e = \beta^o$. So it should be noted that a HWP of this design will not create a perfect polarization shift of 90° . However, if we have

$$\Delta T = |T_{12}^e T_{23}^e - T_{12}^o T_{23}^o| \approx 0 \quad (34)$$

then we have a device that does create the necessary phase retardation and gets us very close to our desired functionality of a 90° polarization shift.

We have not included reflections in our discussion so far, and this was because the base functionality of the HWP was being designed. But, we know that because this is a two interface device, that there are an infinite number of reflections that decrease in amplitude between the two boundaries. It should be mentioned that we are not considering the curved boundary of the device as it is assumed that the incident plane wave does not fully cover the plate of the device.

Picking up from where we left off, if we consider the reflected light from the boundary $z = L$, we find that the reflected field in $\hat{\mathbf{x}}$ is given by

$$E_{x,2}^{tr}(z) = \frac{E_0}{\sqrt{2}} e^{-j\beta^e L} T_{12}^e \Gamma_{23}^e e^{j\beta^e(z-L)} \quad (35)$$

When we consider the reflection of this $-\hat{\mathbf{z}}$ propagating wave on the 1-2 boundary, and use the fact that if the material in region 3 is the same as region 1 ($\Gamma_{21}^e = \Gamma_{23}^e$), we find

$$E_{x,2}^{trr}(z) = \frac{E_0}{\sqrt{2}} e^{-j2\beta^e L} T_{12}^e (\Gamma_{23}^e)^2 e^{-j\beta^e z} \quad (36)$$

Then, if we consider the transmission of this wave through the 2-3 boundary, we find

$$E_{x,3}^{trrt}(z) = \frac{E_0}{\sqrt{2}} e^{-j3\beta^e L} T_{12}^e (\Gamma_{23}^e)^2 T_{23}^e e^{-j\beta_0(z-L)} \quad (37)$$

We could repeat this process indefinitely, but it can be seen that each trip through the uniaxial material imparts a further phase shift on the propagating wave, which is undesirable. But, these phase shifted reflections are decreasing in amplitude $\Gamma_{23}^e < 1$. Fortunately, we do not need to replicate this process to evaluate the $\hat{\mathbf{y}}$ components of the field as we can simply replace all extraordinary coefficients (T^e, Γ^e, β^e) with their respective ordinary components and the problem is solved. Hence

$$E_{y,3}^{trrt}(z) = \frac{E_0}{\sqrt{2}} e^{-j3\beta^o L} T_{12}^o (\Gamma_{23}^o)^2 T_{23}^o e^{-j\beta_0(z-L)} \quad (38)$$

Looking at the relationships between Equations (33), (31), (37), and (38) we see that, because we have a relatively simple problem, it is possible to neatly represent the total output field in $\hat{\mathbf{x}}$ compactly as a series

$$E_{x,3}(z) = \frac{E_0}{\sqrt{2}} e^{-j(\beta_0(z-L))} \sum_{n=0}^{\infty} T_{12}^e (\Gamma_{23}^e)^{2n} T_{23}^e e^{-j(2n+1)[\beta^o L + \pi(2m+1)]} \quad (39)$$

And for the output field in $\hat{\mathbf{y}}$ we obtain

$$E_{y,3}(z) = \frac{E_0}{\sqrt{2}} e^{-j(\beta_0(z-L))} \sum_{n=0}^{\infty} T_{12}^o (\Gamma_{23}^o)^{2n} T_{23}^o e^{-j(2n+1)\beta^o L} \quad (40)$$

We can repeat this analysis to find a series solution for $E_{x,2}(z)$ and $E_{y,2}(z)$ to find

$$\begin{aligned} E_{x,2}(z) &= \frac{E_0}{\sqrt{2}} T_{12}^e \sum_{n=0}^{\infty} (\Gamma_{23}^e)^{2n} e^{-j2n[\beta^o L + \pi(2m+1)]} e^{-j\beta^e z} \\ &\quad + (\Gamma_{23}^e)^{2n+1} e^{-j(2n+1)[\beta^o L + \pi(2m+1)]} e^{j\beta^e (z-L)} \end{aligned} \quad (41)$$

and

$$\begin{aligned} E_{y,2}(z) &= \frac{E_0}{\sqrt{2}} T_{12}^o \sum_{n=0}^{\infty} (\Gamma_{23}^o)^{2n} e^{-j2n\beta^o L} e^{-j\beta^o z} \\ &\quad + (\Gamma_{23}^o)^{2n+1} e^{-j(2n+1)\beta^o L} e^{j\beta^o (z-L)} \end{aligned} \quad (42)$$

For the case of the HWP it should be noted that the round trip reflections will always yield $-\hat{\mathbf{x}}$ from the term $e^{-j(2n+1)\pi(2m+1)} = -1$ for any n , but the fields at $z = L$ will keep being phase shifted by the factor of $e^{-j(2n+1)\beta^o L}$ for each round trip (n can be thought of as the number of round trips after first contact with the 2-3 boundary). These phase delays will cause interference at the output, but are not a strong concern if $(\Gamma_{23}^e)^{2n} \ll 1$ and $(\Gamma_{23}^o)^{2n} \ll 1$. We will discuss this further when we evaluate a designed quartz HWP. Furthermore, it should be noted that the waveplate will only cause a 90° polarization shift if the incident light is polarized roughly $\pm 45^\circ$ in the xy plane. This is satisfactory for most HWP applications. Lastly, the output $\mathbf{H}(z)$ field for the HWP is given by applying the impedance in region 3 to Equations (39), (40) [1]

$$\mathbf{H}_3(z) = \frac{1}{\eta_0} \mathbf{E}_3(z) \quad (43)$$

3.2. Quarter-Waveplate Design

Now that we have introduced the HWP design, we will now design the QWP with the same setup (Figure 1). To turn LP incident light into RHCPL or LHCPL light we want to delay the phase of the $\hat{\mathbf{x}}$ field by a phase of $\pi/2$ or $-\pi/2$. We see that we have already provided the equations necessary to perform this task, the only difference we must make here is that we must change Equation (31) to be

$$L(\beta^e - \beta^o) = (2m + 1) \frac{\pi}{2} \quad \text{for } \forall m \in \mathbb{Z} \quad (44)$$

depending on whether m is odd or even we will obtain right- or left-handed circularly polarized light. The analysis we performed to find $\mathbf{E}_3(z)$ is also still valid, but the phase shift of the light at the output will be different. We can rewrite Equations (39) and (39) to be

$$E_{x,3}(z) = \frac{E_0}{\sqrt{2}} e^{-j(\beta_0(z-L))} \sum_{n=0}^{\infty} T_{12}^e (\Gamma_{23}^e)^{2n} T_{23}^e e^{-j(2n+1)[\beta^o L + (2m+1)\pi/2]} \quad (45)$$

and

$$E_{y,3}(z) = \frac{E_0}{\sqrt{2}} e^{-j(\beta_0(z-L))} \sum_{n=0}^{\infty} T_{12}^o (\Gamma_{23}^o)^{2n} T_{23}^o e^{-j(2n+1)\beta^o L} \quad (46)$$

respectively. We will omit the reflected fields as we have already solved them in the previous section, and we care more about how these reflected fields degrade the output field, instead of their equations. Equation (43) still provides the relationship between the $\mathbf{E}_3(z)$ and $\mathbf{H}_3(z)$ fields in medium 3. From Equation (45) it can be seen that for even n the \hat{x} output field is shifted by a factor of $-j = e^{-j\pi/2}$ relative to the phase of the same n \hat{y} field. For odd n , this becomes a factor of $j = e^{-j\pi/2}$. This means that the reflections flip between right-handed and left-handed. Just as before, each round trip reflection adds an additional phase of $e^{-j2\beta^o L}$.

3.3. Designed Waveplates

Now that we have rigorously solved for the output fields $\mathbf{E}_3(z)$ and $\mathbf{H}_3(z)$, we are able to design a HWP and QWP using quartz. The parameters used for this design are shown in Table 1. The computed transmission and reflection coefficients are shown in Table 2.

λ (nm)	ϵ^e	ϵ^o	β^e (μm^{-1})	β^o (μm^{-1})	η^e (Ω)	η^o (Ω)
590	2.4130	2.3847	16.543	16.445	242.5	244.0

Table 1. Table of parameters for waveplate design. Relative permittivity computed from [5]. Parameters β^e , β^o , η^e , and η^o were determined from the relative permittivities.

Γ_{12}^e	Γ_{12}^o	Γ_{23}^e	Γ_{23}^o	T_{12}^e	T_{12}^o	T_{23}^e	T_{23}^o
-0.217	-0.214	0.217	0.214	0.783	0.786	1.217	1.214

Table 2. Table of computed transmission and reflection coefficients.

To evaluate the performance of the designed devices we introduce the ratio of the $n = 1$ (\mathbf{E}_3^{trrt}) reflected power to the $n = 0$ (\mathbf{E}_3^{tt}) power

$$R \% = \frac{|\mathbf{E}_3^{trrt}|^2}{|\mathbf{E}_3^{tt}|^2} \cdot 100 = \frac{[T_{12}^e(\Gamma_{23}^e)^2 T_{23}^e]^2 + [T_{12}^o(\Gamma_{23}^o)^2 T_{23}^o]^2}{[T_{12}^e T_{23}^e]^2 + [T_{12}^o T_{23}^o]^2} \cdot 100 \quad (47)$$

The value of $R \%$ will give us a sense of how well performing our designed device is. If $R \%$ is low, further reflections will be even lower and can be neglected. The \mathbf{E}_3^{trrt} field will cause the greatest degradation in performance.

Table 3 shows the determined values of L for $m = 1$ and $m = 3$ as well as the discussed performance evaluating parameters. Again, m could be any integer, so these are only highlighting some of many possible lengths for the waveplates to be. It can be seen that changing the length of the device has no impact on ΔT nor $R \%$.

Figures 2 and 3 show the fields $\vec{\mathcal{E}}_1^i(z; t = 0)$, $\vec{\mathcal{E}}_2^t(z; t = 0)$, and $\vec{\mathcal{E}}_3^{tt}(z; t = 0)$ for both the HWP and QWP respectively. The discontinuities at $z = 0$ and $z = L$ arise from the fact that the reflected fields are not considered. The BC require that the tangential components of the all fields be continuous at the boundary, without considering the reflected waves our plot simply would not show this. Figure 4 shows the output field $\vec{\mathcal{E}}_{x,3}(z; t = 0)$ with higher order reflections considered. It can be seen that reflections beyond $\vec{\mathcal{E}}_{x,3}^{trrt}(z; t = 0)$ do not have much impact on the phase of the output field.

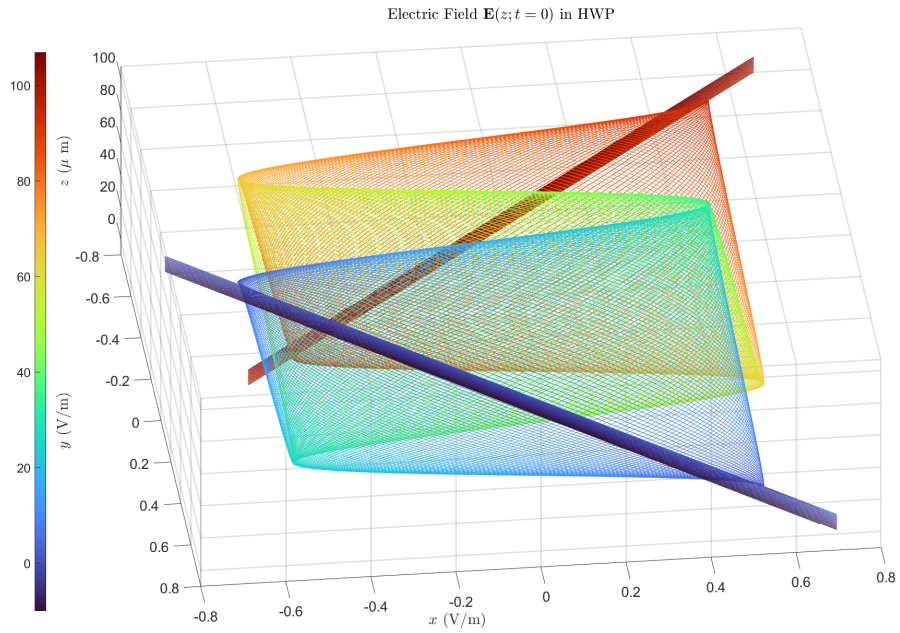


Fig. 2. Forward propagating Electric Field before, inside, and after a quartz HWP, $L = 96.933\mu\text{m}$ and $m = 1$. Color bar helps visualize propagation in z . Reflections not considered, discontinuities of $\vec{\mathcal{E}}(z; t = 0)$ would vanish they were.

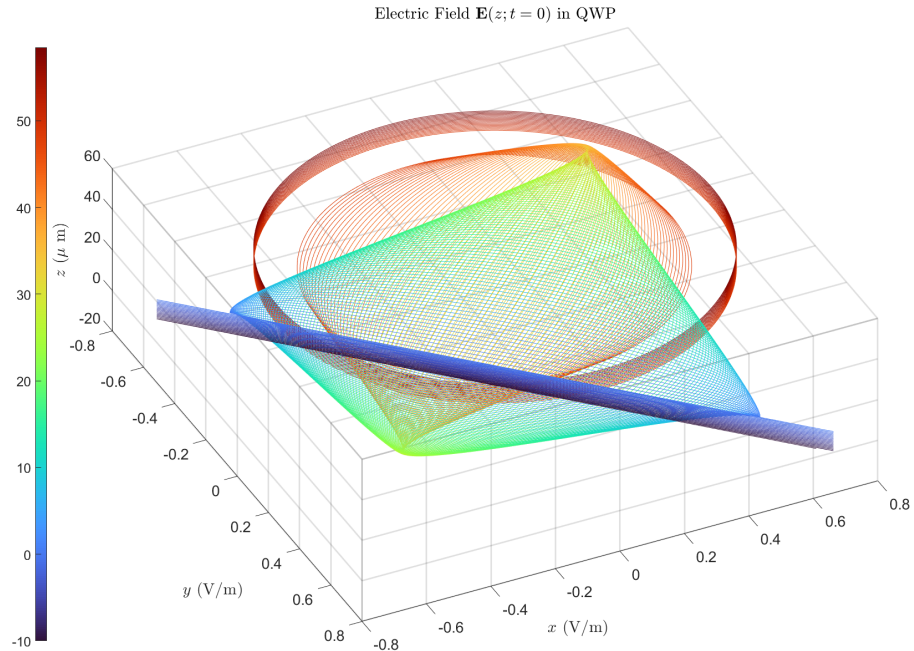


Fig. 3. Forward propagating Electric Field before, inside, and after a quartz QWP, $L = 48.4667\mu\text{m}$ and $m = 1$. Color bar helps visualize propagation in z . Reflections not considered, discontinuities of $\vec{\mathcal{E}}(z; t = 0)$ would vanish they were.

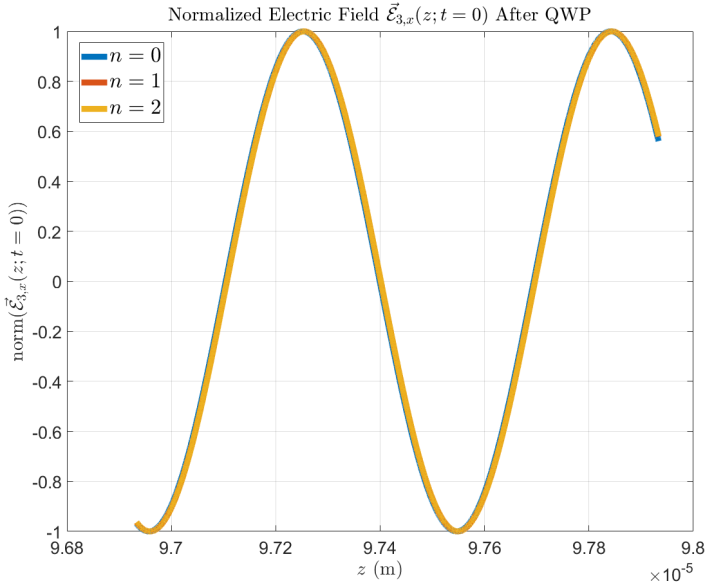


Fig. 4. Plot of the normalized output field $\vec{\mathcal{E}}_{x,3}(z; t = 0)$ for $z > L$ with higher order reflections considered to show the phase shift is minimal. $n = 0$ is the $\vec{\mathcal{E}}_{x,3}^{tt}(z; t = 0)$ field, $n = 1$ is the field given by $\vec{\mathcal{E}}_{x,3}^{tt}(z; t = 0) + \vec{\mathcal{E}}_{x,3}^{trrt}(z; t = 0)$ and so on.

Plate Type	L (μm)	m	ΔT	$R\%$
HWP	96.933	1	0.001	0.215%
HWP	226.178	3	0.001	0.215%
QWP	48.467	1	0.001	0.215%
QWP	113.089	3	0.001	0.215%

Table 3. Designed quantities and performance characterization quantities

4. Discussion

Now that we have designed a HWP and QWP for normally incident light, provided some crude metrics to evaluate its performance, and plotted the fields inside of the waveplates, we will further discuss their performance and utility.

4.1. Oblique Incidence

Our analysis to this point has focused on the case of normal incidence, but what if we desire our device to perform in the case of oblique incidence? Well, unfortunately, a waveplate of this design is not able to have its intended effects for the case of oblique incidence. We saw earlier that we needed to employ two different transmission and reflection coefficients for the fields in \hat{x} and \hat{y} . In our example, the extraordinary and ordinary coefficients respectively. So to consider oblique incidence, we must also apply Snell's law twice as well, shown in Equations (48) and (49).

$$\theta_t^e = \sin^{-1} \left(\frac{\beta_0}{\beta^e} \sin(\theta_i) \right) \quad (48)$$

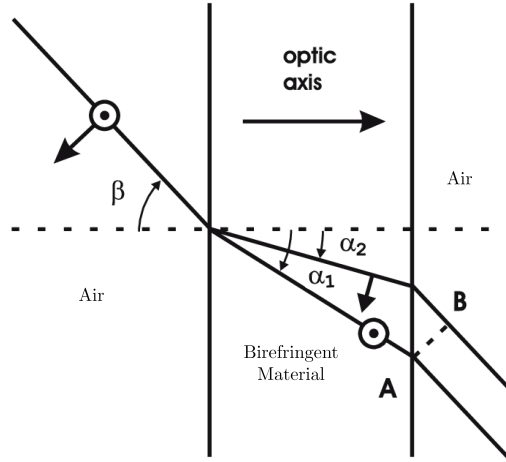


Fig. 5. We obtain two spatially separated propagating fields when we consider the case of oblique incidence on a birefringent material [6].

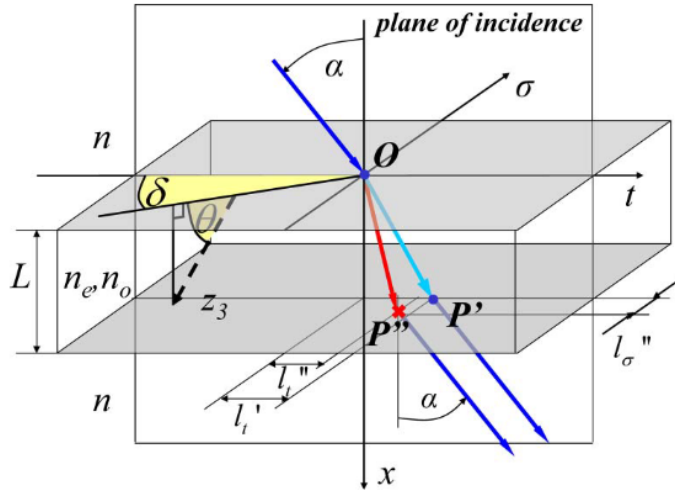


Fig. 6. “Ordinary and extraordinary transmission through a uniaxial plane-parallel plate immersed in an isotropic medium. θ is the angle between the optical axis and the interface. δ is the angle between the plane of incidence and the optical axis projection on the interface.” α is the angle of incidence. [7].

$$\theta_t^o = \sin^{-1} \left(\frac{\beta_0}{\beta^o} \sin(\theta_i) \right) \quad (49)$$

We know that β^e and β^o are often similar for many materials, but still differ. As such, it can be seen that for cases of very shallow incidence, $\theta_i \approx 0^\circ$ that $\sin(\theta_i) \approx 0$ which means that despite the small difference between β^e and β^o the waveplate will still function mostly as intended. In the case of the QWP the slightly elliptically polarized output field would become even more elliptically polarized as the slightly different angles of refraction would cause a slight additional phase shift on one of the fields. But, for the case where $\sin \theta_i$ is not approximately zero, we see that Equations (48) and (49) yield very different angles of transmission. Figure 5 shows what the transmitted fields would look like. We see that the transmitted fields become more spatially separated as they

propagate through the anisotropic material, and that they are spatially separated at the output. We call this effect, when we have two refracted EM waves that originate from one incident ray, birefringence. Furthermore, we call the materials that this effect happens in *birefringent materials*. Anisotropic materials usually exhibit this property because their permittivities are directionally dependent.

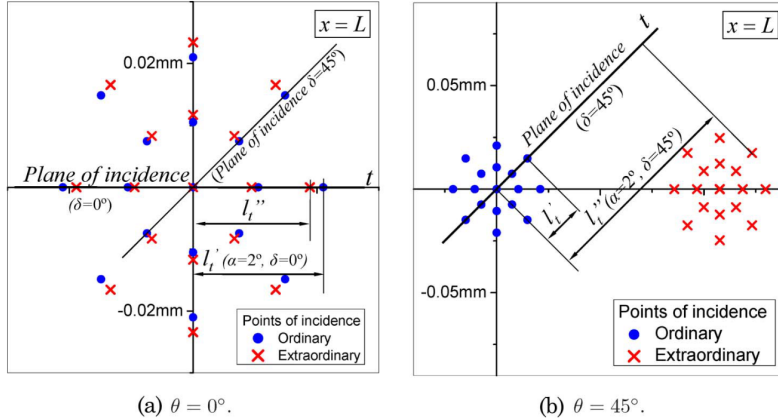


Fig. 7. Spatial separation of the ordinary and extraordinary rays at the output plane of a calcite plate where the angle of incidence normal to the surface is given by α and the azimuthal angle δ relative to the optical axis of the device, shown in Figure 6 (a) the case where the materials crystalline structure is oriented with an ordinary and extraordinary axis parallel to the surface $\theta = 0^\circ$ and (b) the case of the crystalline structure being aligned with $\theta = 45^\circ$ [7].

It should be noted that in our example, if we had an obliquely incident field, where its E field was present in both \hat{x} and \hat{z} , that there would only be one transmitted wave. While we already noted that a field purely in \hat{y} would not have its polarization changed by the waveplate, if it was obliquely incident, it would also not create multiple waves inside of the uniaxial material because the permittivities in the \hat{y} and \hat{z} are the same.

Understanding how waveplates function with oblique incidence is of particular interest to researchers and engineers. There are many applications where polarization transformations are desired, but ensuring normal incidence may not be possible.

Figure 6 shows the variables for plane wave incidence on a birefringent material as described in *Phase shift formulas in uniaxial media* which will be used in to discuss Figure 7 [7]. Part (a) in Figure 7 shows that for slight obliquely incident light $\alpha = 2^\circ$ with the material having its optical axis being normal to its surface (the designed case that we did in this report) we see that for different orientations of this obliquely incident light (described by δ) the ordinary and extraordinary rays do not align at the output plane of the device. Furthermore, if we change the optical axis of the device, which would correspond to misalignment of the permittivity tensor, we see that the device performance completely breaks down: Figure 7-b. As expected, the birefringent properties of the anisotropic material cause the fields to spatially diverge substantially. This paper supports the need to make the design choices articulated in the design portion of this report. Furthermore, the phase delay for a desired quarter-wave plate $\Delta\phi(\alpha, \delta)$ is shown in Figure 8. For incident angles of $\alpha > 4^\circ$ we start to notice more pronounced differences between the desired phase shift of 90° and the actual phase $\Delta\phi(\alpha, \delta)$ [7].

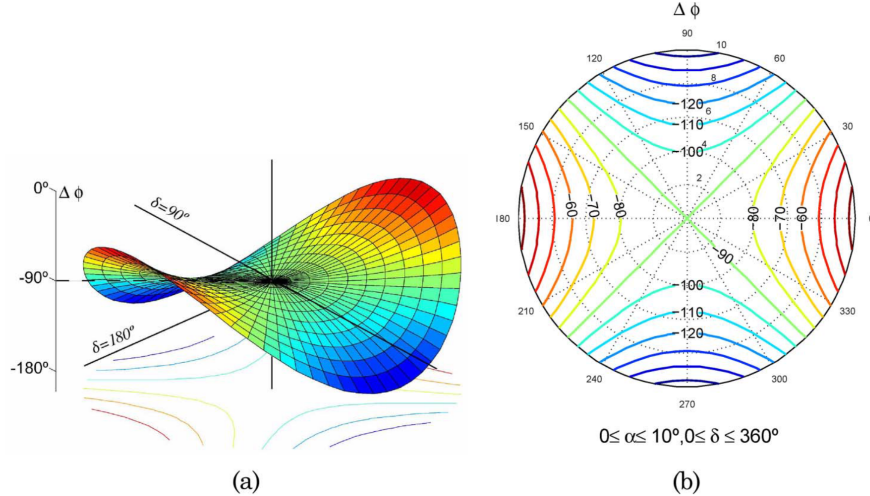


Fig. 8. Oblique incidence phase delay $\Delta\phi(\alpha, \delta)$ at the output plane of a quartz half-waveplate where the angle of incidence normal to the surface is given by α and the azimuthal angle δ relative to the optical axis of the device as shown in Figure 6. On the plots, the azimuthal angle of the coordinate system corresponds to the various angles of δ and the radial direction on the graphs indicates $0^\circ < \alpha < 10^\circ$ [7].

4.2. Anti-Reflective Coatings

Figure 4 and our metric $R\%$ showed that our designed waveplates work fairly well even with the internal reflections of the device. However, to make the output field even more consistent with the desired polarization, anti-reflective coatings could be employed to further diminish the slight phase delay that the round trip reflections cause. These coatings could be placed on both sides of the waveplate to further couple the output field and reduce the reflection coefficients even further. However, with the addition of more interfaces to our device, there are more opportunities for internal reflections, and it becomes impossible to make a neat series solution for the problem. In our design section, we exploited the fact that we can describe each round trip through our device by a phase factor to get our analytical solution, but this becomes too tedious to perform. Such devices would have to be modeled with finite difference time domain method (FDTD) or rigorous coupled wave analysis (RCWA) [8, 9]. Both of these methods are numerical methods to approximate the solutions to Maxwell's equations and while computationally expensive, they are able to solve problems with complex boundary conditions such as a graded index fiber or complex anisotropic materials such as liquid crystals.

4.3. Wavelength Dependence

The design for the QWP and HWP presented in this report neglected to consider the case for an achromatic incident field. For Quartz, an most anisotropic materials, their relative permittivities ϵ^e and ϵ^o are frequency dependent. As such, as the frequency changes the values of β^e and β^o vary—meaning that the neat phase delay factors we related to the length will not work for the whole range of incident frequencies. But if we can live with slight elliptically polarized light in our application, and we choose materials such that β^e and β^o remain relatively unchanged, it is possible to design a device that closely meets the desired performance.

However, we as engineers have more tools at our disposal, it is possible to couple multiple anisotropic materials together to help reduce this chromatic dispersion. “The most common type is crystalline quartz and magnesium fluoride birefringent crystals in an air-spaced design” [10].

By making more complicated designs, we make tradeoffs in our design criteria to make electromagnetic devices that meet the desired operating criteria.

4.4. Liquid Crystals

Liquid crystals are a very different type of anisotropic material that are highly useful for research and consumer applications. Most notable, they are ubiquitous in computer displays. In the display the liquid crystal is used to modulate the polarization of a pixel's back-light such that when the modulated light hits the polarizing film of the display, the brightness of the display's pixels can be independently controlled by modulated the voltage bias on the crystal. A similar technique is used by spatial light modulators (SLM) which are devices that use a pixelated liquid crystal to impart a phase delays on an incident wavefront. In both of these devices, it is the anisotropic properties of the liquid crystal that allows for the light to be modulated. When we apply a bias voltage we are able to change the crystalline structure and therefore alter the optical axis of the material. Information regarding the refractive indices n and therefore the relative permittivities ϵ_r (in the case of non-magnetic liquid crystals) is well documented by Jun Li in his PHD thesis [11]. The author had initially wanted to model liquid crystal based devices, but with no background in anisotropy this proved to be difficult. Hence, our discussion almost entirely focused on uniaxial media, but this section on liquid crystals was included for some additional background on anisotropic materials.

5. Conclusion

This paper has provided a discussion on electromagnetic fields in uniaxial media, with a focus on designing waveplates for changing the polarization of an incident electromagnetic wave. The theoretical background was presented, and analytical solutions were derived for half-waveplate and quarter-waveplate designs using a quartz crystal for 590 nm normally incident light. The performance of the designed waveplates was evaluated, and the challenges associated with waveplate design were discussed. This paper serves as an introduction into anisotropic electromagnetic device design.

Funding. This research is unfunded.

Acknowledgments. The author thanks T. Saule for his contributions to the author's understanding.

Disclosures. The authors declare no conflicts of interest.

Data availability. L^AT_EX and MATLAB code for this project and its reports can be found on the author's github and are accessible at the following link: <https://github.com/kevinlindstrom/ECE5201>

References

1. C. A. Balanis, *Antenna Theory: Analysis and Design* (Wiley-Interscience, 2005).
2. D. J. Griffiths, *Introduction to Electrodynamics* (Pearson, 2013).
3. P. Beyersdorf, "Coupled mode analysis," <https://www.sjsu.edu/faculty/beyersdorf/Archive/Phys208F07/ch%204-EM%20waves%20in%20anisotropic%20media.pdf>.
4. F. Ran, "Waves in Anisotropic Media," <https://courses.cit.cornell.edu/ece303/Lectures/lecture17.pdf> (2007).
5. G. Ghosh, "Dispersion-equation coefficients for the refractive index and birefringence of calcite and quartz crystals," Opt. Commun. **163**, 95–102 (1999).
6. A. Lutich, M. Danailov, s. Volchek, V. Yakovtseva, V. Sokol, and S. Gaponenko, "Birefringence of nanoporous alumina: Dependence on structure parameters," Appl. Phys. B **84**, 327–331 (2006).
7. F. Veiras and L. Perez, "Phase shift formulas in uniaxial media: an application to waveplates," Opt. Soc. Am. **t** (2010).
8. A. Taflove and S. C. Hagness, *Computational Electrodynamics: The Finite-Difference Time-Domain Method* (Artech House, 2000), 3rd ed.

9. P.-J. Chen, P. Engel, A. Mazur, C. Abélard, and H. P. Urbach, "Finite element method for 3D optical modeling of liquid crystal on silicon spatial light modulator," in *Emerging Liquid Crystal Technologies XV*, vol. 11303 L.-C. Chien and D. J. Broer, eds., International Society for Optics and Photonics (SPIE, 2020), p. 1130308.
10. "Introduction to waveplates," <https://www.newport.com/n/introduction-to-waveplates>.
11. J. Li, "Refractive Indices Of Liquid Crystals And Their Applications In Display And Photonic Devices ," Ph.D. thesis, University of Central Florida (2005).